

Anomalous behavior of spin wave resonances in $\text{Ga}_{1-x}\text{Mn}_x\text{As}$ thin films

T. G. Rappoport,¹ P. Redliński,¹ X. Liu,¹ G. Zaránd,² J. K. Furdyna,¹ and B. Jankó¹

¹*Department of Physics, University of Notre Dame, Notre Dame, IN 46556*

²*Institute of Physics, Budapest University of Technology and Economics, H-1521 Budapest, Hungary*

(Dated: October 30, 2018)

We report ferromagnetic and spin wave resonance absorption measurements on high quality epitaxially grown $\text{Ga}_{1-x}\text{Mn}_x\text{As}$ thin films. We find that these films exhibit robust ferromagnetic long-range order, based on the fact that up to seven resonances are detected at low temperatures, and the resonance structure survives to temperatures close to the ferromagnetic transition. On the other hand, we observe a spin wave dispersion which is *linear* in mode number, in qualitative contrast with the quadratic dispersion expected for homogeneous samples. We perform a detailed numerical analysis of the experimental data and provide analytical calculations to demonstrate that such a linear dispersion is incompatible with uniform magnetic parameters. Our theoretical analysis of the ferromagnetic resonance data, combined with the knowledge that strain-induced anisotropy is definitely present in these films, suggests that a spatially dependent magnetic anisotropy is the most likely reason behind the anomalous behavior observed.

PACS numbers: 75.50.Pp, 76.50.+g, 75.30.Ds, 75.30.Gw

I. INTRODUCTION

There has been great deal of interest in elucidating the properties of $\text{Ga}_{1-x}\text{Mn}_x\text{As}$ and other diluted magnetic semiconductors (DMSs) during the past several years. The intense research on these materials is partly motivated by the fact that they hold promise as building blocks of “spintronic” semiconductor devices^{1,2,3}. Indeed, the incorporation of magnetic properties in semiconductor heterostructures can, in principle, lead to the development of new devices that manipulate both the spin and the charge degrees of freedom of the carriers. Due to its compatibility with conventional electronic devices, $\text{Ga}_{1-x}\text{Mn}_x\text{As}$ is one of the most readily usable alloy systems for exploring spintronic prototypes. However, these materials exhibit a series of fascinating strong correlation phenomena that are not yet fully understood, such as a metal-insulator transition, field-induced ferromagnetism, and magnetoresistance³. Before any applications become possible, it is necessary to provide a detailed description of both electronic and magnetic structure and properties of this class of materials. Investigating the magnetic properties of the ferromagnetic ground state in $\text{Ga}_{1-x}\text{Mn}_x\text{As}$, with Curie temperatures as high as $T_c \sim 160\text{K}$, is therefore especially important.

Given the fact that DMSs are synthesized in film form by using molecular-beam epitaxy (MBE), ferromagnetic resonance spectroscopy (FMR) is the most suitable experimental probe for studying the dynamics of the ferromagnetic order parameter, that also allows for the spectroscopy of the spin wave excitations. FMR is a powerful technique to study magnetic properties in magnetic thin films⁴ and has already been used by several groups in the magnetic characterization of the $\text{Ga}_{1-x}\text{Mn}_x\text{As}$ films^{5,6}. The same technique can be used to obtain the resonance fields of the spin wave modes in a thin film. Extracting the various magnetic parameters influencing the spin excitations is essential for gaining complete control of

the magnetic properties of DMS films with an eye on successful future applications, such as spin injection and manipulation.

The main objective of this paper is to provide a self-consistent picture of the properties of spin wave excitations based on a comparison of experimental results and theoretical calculations. The theory of spin wave resonance (SWR) has been developed four decades ago by Kittel⁷, who also pointed out that FMR measurements are capable of detecting several modes of the magnetic excitations in ferromagnetic thin films. For an external magnetic field normal to the surface of a homogeneous film he finds the following resonance condition for spin waves pinned at its boundaries.

$$H_n = H_0 - D \left(\frac{\pi}{L}\right)^2 [(n+1)^2 - 1], \quad (1)$$

where H_n is the external field value (at fixed external radiation frequency) where the n -th SWR mode is observed, H_0 is the magnetic field that corresponds to the ferromagnetic resonance, L is the sample thickness and the constant D is proportional to the stiffness constant defined in Sec. III⁸.

In this paper we report the observation of such spin wave resonances in $\text{Ga}_{1-x}\text{Mn}_x\text{As}$. These experiments provide a direct proof for true *long-ranged ferromagnetic order* in $\text{Ga}_{1-x}\text{Mn}_x\text{As}$. Surprisingly, the spin waves which we observe exhibit a somewhat unusual behavior: We find a spin wave spectrum with $H_n \sim n$. A recent work by Goennenwein and collaborators⁹ reported $H_n \sim n^{2/3}$. Both results are in qualitative disagreement with Eq. (1), which states that for a homogeneous film the resonance field H_n of the n^{th} mode should be proportional to $\sim n^2$. We trace back the origin of the anomalous dispersion to the magnetic properties of $\text{Ga}_{1-x}\text{Mn}_x\text{As}$ thin films, and find that in order to understand the anomalous spin wave dispersion, it is *crucial* to allow the

magnetic parameters inside the film to depend on the distance from the interface. In principle, such inhomogeneity in the profile of magnetization, spin stiffness, or magnetic anisotropy⁹ could all result in such an anomaly. However, our experimental and theoretical results presented in this paper point towards the presence of uniaxial anisotropy and/or spin stiffness that depends on the distance z from the surface of the film. More specifically, we find that our resonance experiments can be well understood by assuming a uniaxial magnetic anisotropy with a quadratic dependence on the distance z from the Ga_{1-x}Mn_xAs/GaAs interface. The presence of strong magnetic anisotropy in Ga_{1-x}Mn_xAs and In_{1-x}Mn_xAs epitaxial films has already been clearly demonstrated by a series of experiments^{5,6,10,11,12,13}, which also indicate that the magnetic anisotropy depends on the lattice mismatch between the substrate and the DMS layer.

This paper is organized as follows: In Section II we present the experimental results for a group of as-grown and annealed Ga_{1-x}Mn_xAs samples and discuss briefly the position, intensity and linewidth of the observed resonance peaks. In Section III we present a general spin wave equation of motion that allows for the variation of the magnetization and magnetic anisotropy along the film thickness, and discuss our numerical calculation for the position and intensity of the resonance peaks. Finally, in Section IV we compare the experimental results with the theoretical calculations and discuss the possible explanations for the inhomogeneity of the magnetic anisotropy.

II. EXPERIMENTAL RESULTS

Recently, a systematic study of the fundamental FMR mode has been reported for a series of Ga_{1-x}Mn_xAs films grown on various substrates⁵. The dependence of the FMR position on the angle between the applied magnetic field and the crystallographic axes of the sample was carefully documented, and detailed information has been obtained on the magnetic anisotropy and its variation with temperature. The uniaxial and cubic anisotropies determined experimentally generally corroborate with earlier theoretical predictions^{11,12}. In this paper the same experimental technique is used to study spin wave resonances (SWRs) in thin Ga_{1-x}Mn_xAs films.

Although DMSs have a very low concentration of magnetic atoms, and these system are often described in terms of percolation¹⁴ and impurity band models^{15,16}, it was possible to observe SWR spectra with up to seven spin wave modes^{9,17}, demonstrating that real long-range order develops in these materials.

The three Ga_{1-x}Mn_xAs thin films analyzed in this paper have previously been studied by Sasaki *et al.*, who observed both the SWR and the FMR lines. Their initial work concentrated on the uniform mode (the FMR line), and they used this feature to investigate the overall magnetic anisotropy in Ga_{1-x}Mn_xAs films⁵. All the

Thickness	Annealed [nm]	T [K]	H_{max} [Oes]	M [$\frac{\text{emu}}{\text{cm}^3}$]	T_c [K]	ΔH [Oes]
200	No	4	7820	17.9	65	200 ± 20
	No	40	7600	9.4	65	170 - 200 ± 20
	Yes	4	8700	25	95	120 - 220 ± 20
150	No	4	8350	17.5	65	230 ± 20
	No	40	7920	9.4	65	230 ± 20
	Yes	4	8820	23	90	180 - 230 ± 20
100	No	4	8110	17.5	65	150 ± 20
	No	40	7740	9.4	65	200 ± 20
	Yes	4	9050	25	100	110 ± 20

TABLE I: Experimental parameters extracted from, and used in the theoretical analysis of, the spectra of three Ga_{0.924}Mn_{0.076}As samples of different thicknesses, pre- and post-annealing. H_{max} is the resonance field of the highest (ferromagnetic resonance) peak, M is the static magnetization measured by SQUID, T_c is the critical temperature, and ΔH is the linewidth. When the width varies with the mode number (see text), the range of linewidths is given.

samples were grown by low temperature molecular beam epitaxy (LT-MBE) on semi-insulating GaAs substrates. The Mn concentration $x = 0.076$ was determined by x-ray diffraction, and the Curie temperature and dependence of magnetization dependence on applied magnetic field and temperature were obtained by superconducting quantum interference device (SQUID) measurements. The FMR and SWR measurements were carried out using a 9.46 GHz microwave spectrometer.

The dc magnetic field H_{ext} was oriented perpendicular to the film plane (see Fig. 1). As a result of the lattice mismatch between the substrate and the Ga_{1-x}Mn_xAs films, the samples exhibit compressive strain in the sam-

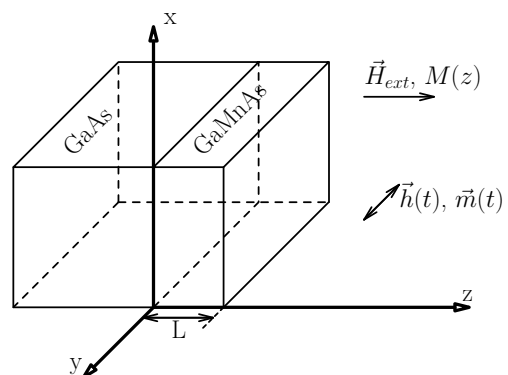


FIG. 1: Schematic diagram of the experimental geometry. The Ga_{1-x}Mn_xAs film is grown on a thick GaAs substrate. A large constant magnetic field \vec{H}_{ext} is applied in the \hat{z} direction: $\vec{H}_{ext} \parallel \hat{z}$. This field produces a large magnetization $\vec{M}(z)$ which points predominantly in the \hat{z} direction. Additionally, a small external microwave magnetic field $\vec{h} \perp \vec{H}_{ext}$ produces a small harmonically-varying perturbation in magnetization, $\vec{m} \perp \hat{z}$

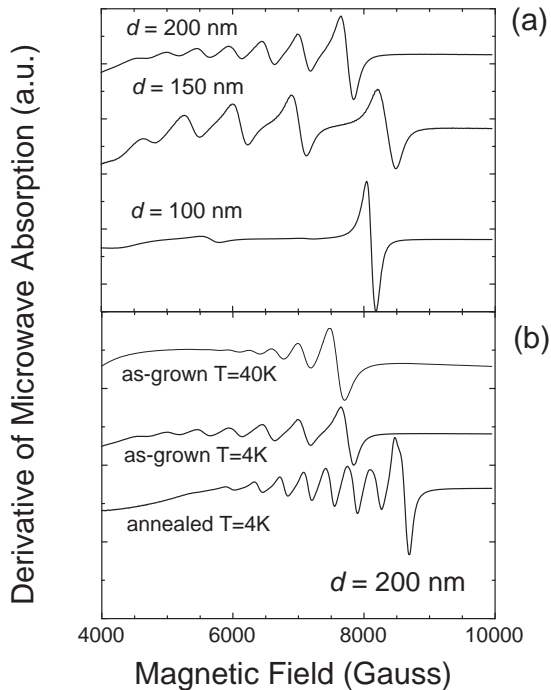


FIG. 2: (a) FMR and SWR absorption spectra for as-grown $\text{Ga}_{0.924}\text{Mn}_{0.076}\text{As}$ samples of different thickness (100 nm, 150 nm and 200 nm) at $T=4$ K. (b) FMR and SWR spectra for the 200 nm thick $\text{Ga}_{0.924}\text{Mn}_{0.076}\text{As}$ sample for different temperatures, before and after annealing.

ple plane, which leads to a strong uniaxial anisotropy. Consequently, in the absence of the external field the magnetization lies in the plane parallel to the film. However, the applied static field at which FMR and SWRs are observed is strong enough to align the magnetization perpendicular to the sample surface. After measuring the SWR in the as-grown samples, we annealed them for 60 minutes. As a result, the Curie temperature T_c was increased by about $\sim 40\%$ and the magnetization by $\sim 25\%$. Table I summarizes some of the characteristic properties of three representative $\text{Ga}_{1-x}\text{Mn}_x\text{As}$ samples. The values listed in the table were extracted from SQUID, FMR and SWR measurements. Clearly, the annealing process has a profound effect not only on the critical temperature and magnetization of the films, but on practically all characteristics of the the ferromagnetic and spin wave resonances, including the temperature and thickness dependence of the resonance position and linewidth. In order to obtain more insight into the behavior of these materials, we now proceed to evaluate the actual FMR spectra before and after annealing.

Fig. 2 shows typical examples of the observed spectra. The main trends and qualitative features of these data can be effectively conveyed if the position and linewidth of the resonance features are plotted as a function of the

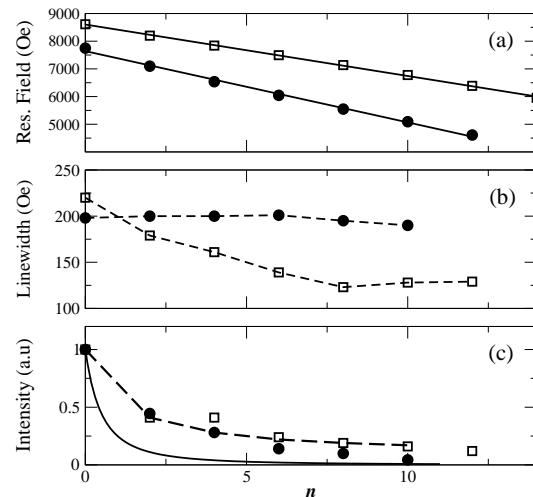


FIG. 3: Experimentally observed $T = 4$ K SWR mode positions (a), linewidths (b) and peak intensities (c) for the 200 nm thick $\text{Ga}_{0.924}\text{Mn}_{0.076}\text{As}$ sample before (open circles) and after (open squares) annealing as a function of mode index n . (a) the solid lines show the linear fitting for the experimental data. (c) The dotted line connects the theoretical result for the normalized peak intensities. Note that this calculation was done *with no fitting parameters* (see text). Odd modes are not observed experimentally, as their amplitudes are much smaller compared to those of the even modes.

mode number. We label the largest resonance at the highest field (the uniform FMR mode) as $n = 0$, and the SWR modes as $n = 1, 2, 3, \dots$, where the increasing mode index corresponds to decreasing resonance field. The results of this procedure are shown in Fig. 3. The distance between SWR modes increases for thinner samples. This is in accordance with the simple picture, that these resonances are standing waves of magnetization trapped between the two interfaces of a uniform thin film, and that the level spacing between successive standing wave modes increases with decreasing geometrical size of the 'resonator cavity'. However, from this simplistic picture also follows that the resonances must depend quadratically on the mode index, in accordance with Kittel's equation, (1). This expectation fails spectacularly in our $\text{Ga}_{1-x}\text{Mn}_x\text{As}$ thin films. As one can see in Fig. 3 for the 200 nm thick as-grown and annealed samples, in spite of the fact that we are able to see as many as 7 spin-wave resonances, the SWR mode positions as a function of the mode number do not follow the expected quadratic law. Instead, the resonance fields H_n exhibit a *linear dependence* on the mode index n .

We can also compare the intensity of the resonances with Kittel's predictions. However, to do that we have to keep in mind that the FMR measurement is done with a field modulation lock-in technique, which measures the derivative of the absorption as a function of the applied

magnetic field. The observed peak-to-peak height ΔI_n and peak-to-peak width ΔH_n of the n -th resonance are related to its intensity I_n as¹⁸

$$I_n \sim \Delta I_n \Delta H_n^2 \quad (2)$$

It is rather striking that the linewidth behaves qualitatively differently for annealed and unannealed samples: For the as-grown film the linewidth is independent of n and its value is $\Delta H_n \sim 200$ Oe. For the annealed samples, on the other hand, ΔH_n decreases with n (see Fig. 3.b), which is a typical behavior of metallic thin films¹⁹. This change to more conventional behavior in the resonance linewidth corroborates the observation that the annealed samples are more metallic than the as-grown samples: resistivity decreases upon annealing, consistent with an increase in the density of mobile charge carriers²⁰. On the other hand, the peak intensities *remain* anomalous despite the annealing. The extracted intensities I_n are shown in Fig. 3.c. They follow a similar law for both the annealed and unannealed samples, and the decrease of the successive intensities is much slower than the $I_n \propto 1/(n+1)^2$ dependence predicted by Kittel.

Clearly, based on the qualitative and quantitative experimental observations made above, the $\text{Ga}_{1-x}\text{Mn}_x\text{As}$ films do not behave as homogeneous ferromagnetic thin films. The first attempt to explain this behavior is due to Sasaki *et al.*^{17,21} who, inspired by the work of Portis²², suggested a picture where the magnetization inside the ferromagnetic thin film is not homogeneous in the direction perpendicular to the plane of the film. Although such inhomogeneity could explain qualitatively the linear dependence of successive SWR positions on n , the gradient of composition required to fit the data is unrealistically large, and recent neutron reflectivity measurements²³ do not support this degree of variation of magnetization across the sample. An alternative model is therefore needed for comparing experiment and theory. We present such a theoretical analysis in the following section, which will retain in spirit the approach of Refs. 17,21 in that we also propose inhomogeneity in

magnetic parameters along the thickness of the sample as the main reason behind the observed anomalous behavior of the SWR positions. However, in our theoretical framework – in addition to a gradient of magnetization – we also allow for a variation in magnetic anisotropy and spin stiffness. One of the attractive features of our approach is that – once the anisotropy profile has been determined to fit the resonance positions – it allows for a *parameter-free evaluation* of the normalized peak intensities (see the points connected by dashed lines in Fig. 3.c.). The results are in excellent agreement with those extracted from the experiment for *both* as-grown and annealed samples²⁴. This agreement in particular gives us confidence that the theoretical model and numerical analysis which we present below gives an essentially accurate description of the FMR and SWR experiments in $\text{Ga}_{1-x}\text{Mn}_x\text{As}$.

III. THEORETICAL APPROACH

A. Semiclassical spin wave equations

It is well accepted that the magnetism of the $\text{Ga}_{1-x}\text{Mn}_x\text{As}$ is due to indirect interaction between Mn spins mediated by holes^{15,25,26,27}. Although this system contains considerable positional disorder – which, combined with spin-orbit effects, may lead to non-collinear ground states^{27,28} – it appears that on larger length scales, relevant for the long wavelength collective modes of the ferromagnetic order parameter, these DMS materials behave as conventional ferromagnets²⁹. In the following we will therefore neglect many of the complications which are not relevant when dealing with spin waves, and we shall employ the usual semi-classical equations of motion to study spin wave excitations in the absence of damping³⁰.

The first step to derive the semiclassical equations of motion is to construct the free energy functional for the magnetization $\vec{\mathbf{M}}(\mathbf{r})$. For temperatures below the transition temperature T_C this can be expressed as

$$F(\vec{\mathbf{M}}) = \int_V d^3r \frac{A}{M^2} |\nabla \vec{\mathbf{M}}|^2 + \int_V d^3r \frac{K}{M^2} |\vec{\mathbf{M}} \cdot \vec{u}|^2 - \int_V d^3r (\vec{\mathbf{H}}_{ext} - 2\pi \vec{\mathbf{M}}) \cdot \vec{\mathbf{M}}. \quad (3)$$

In Eq. (3), $M = |\vec{\mathbf{M}}|$ denotes the magnetization of the sample at temperature T , and $H_{ext}||\hat{z}$ is the applied dc magnetic field. Every integration runs over the volume V of the film. Note that the free energy functional in Eq. (3) only describes *transverse* fluctuations of the magnetization, and the longitudinal fluctuations are assumed to be negligible, $M = |\vec{\mathbf{M}}| = \text{constant}$.

The first term in Eq. (3) is an exchange free energy, with $A(\mathbf{r})$ denoting the spin wave stiffness, while the sec-

ond term represents - depending on the sign of $K(\mathbf{r})$ - a uniaxial or an in-plane anisotropy energy with respect to direction \vec{u} . The primary source of the anisotropy K is the strain field due to the lattice mismatch between the GaAs substrate and the ferromagnetic $\text{Ga}_{1-x}\text{Mn}_x\text{As}$ film³¹. Since the $\text{Ga}_{1-x}\text{Mn}_x\text{As}$ films discussed throughout this paper were deposited on GaAs, they have an in-plane easy axis which corresponds to $\vec{u} = (0, 0, 1)$ and positive K . We have not included other cubic anisotropy

terms in Eq. (3) because at temperatures they are small compared to $|K|$. Finally, the last term in Eq. 3 is the Zeeman free energy together with the demagnetization energy. Note that all coefficients in Eq. (3) depend on temperature T , and on *spatial coordinates*.

Given the material specifics detailed above, the semi-classical equations of motion can be written as follows:

$$\frac{d\vec{M}(\vec{r}, t)}{dt} = -|\gamma|\vec{M}(\vec{r}, t) \times \vec{H}_{tot}(\vec{r}, t). \quad (4)$$

Here γ is the gyromagnetic ratio, which we approximate by that of the Mn core spins, $\gamma \approx \gamma_e = 2\mu_B/\hbar$. $\vec{H}_{tot}(\vec{r}, t)$ denotes the total effective magnetic field, which can be obtained by taking the functional derivative of the free energy functional, Eq. (3), with respect to the magnetization, $\vec{H}_{tot}(\vec{r}, t) = -\delta F(\{\vec{M}\})/\delta\vec{M}(\vec{r}, t)$. The result at $T = 0$ K temperature is

$$\vec{H}_{tot}(\vec{r}, t) = -\Lambda\nabla^2\vec{M}(\vec{r}, t) - \frac{2K}{M}\hat{z} + \vec{H}_{ext} - 4\pi\vec{M}, \quad (5)$$

where ω_r is the frequency of the microwave radiation. In course of the derivation of Eq. 6 we assumed that only the magnetic anisotropy and the magnetization vary along the Z direction (growth direction) ($H_a = H_a(z)$ and $M = M(z)$), but (as already mentioned after Eq. (5)) that $\Lambda(z) = \Lambda$ is constant. While these assumptions need not be valid in general, we will show below that the experimental data on our DMS films can be well explained by the presence of a spatially-dependent anisotropy field⁹. As mentioned before, a spatially varying magnetization can also reproduce qualitatively the main features of the data¹³, but if one allows only $M(z)$ to vary, we now find by numerically solving Eq. (6) an unrealistic solution that cannot reproduce quantitatively the experimental SWR spectrum. There is yet another possibility, that the exchange constant is itself spatially dependent, $\Lambda = \Lambda(z)$. Given that Λ depends on the carrier concentration, a scenario with a z -dependent exchange constant would, in principle, be consistent with recent experiments of Koeder and coworkers³². While we cannot exclude this possibility, we expect that this would give a spectrum similar to that of the spatially non-uniform magnetization, and therefore a very large spatial dependence of the carrier concentration would be needed to explain the experimental data. We therefore classify this possibility, together with that of spatially-dependent magnetization, as *sub-dominant* mechanisms, which would at most play a secondary role in explaining the features of our resonance experiments. The versatil-

ity of our numerical analysis is clearly evident in evaluating the different scenarios discussed above: our numerical scheme allows us to check all these scenarios against our resonance absorption data and the constraints set by other experiments, and select the most viable one for explaining our FMR and SWR measurements.

$$\vec{H}_a = -\frac{2K}{M}\hat{z}.$$

To compute the spin wave spectrum for a field parallel to \hat{z} we expand the magnetization around its equilibrium value and orientation $M\hat{z}$ and, as we mentioned before, we allow for transverse deviations only: $\vec{M} = M\hat{z} + \vec{m}(\vec{r}, t)$. Assuming periodic time dependence and plane wave character of the *r.f.* magnetization in the x and y directions, $\vec{m}(\vec{r}, t) = [m_x(z)\hat{x} + m_y(z)\hat{y}]e^{i\omega t}e^{ik_x x + ik_y y}$, one obtains the following equation of motion for $m^+(z) \equiv m_x(z) + im_y(z)$ in the long wavelength limit $k_x, k_y \rightarrow 0$:

$$\left\{-\Lambda M \frac{d^2}{dz^2} + 4\pi M(z) - H_a(z) - \Lambda \frac{d^2 M(z)}{dz^2}\right\} m^+(z) = \left(H_{ext} - \frac{\omega_r}{\gamma}\right) m^+(z), \quad (6)$$

Equation (6) has the form of a one-dimensional Schrödinger equation for an electron in a quantum well. If we compare the coefficients in Eq.6 with the Schrödinger equation, we can see that $\hbar^2/(2\Lambda M(z))$ is the analog of the electron mass (in our case it may depend on the position z if M varies with position) and $4\pi M(z) - H_a(z) - \Lambda \frac{d^2 M(z)}{dz^2}$ is the analog of the potential energy $V(z)$. Equation (6) can then be formally written as

$$\left[\frac{p^2}{2m} + V(z)\right]m_n^+(z) = E_n m_n^+(z), \quad (7)$$

where $p = -i\hbar \frac{d}{dz}$ is the momentum operator and $E_n = H_{ext} - \frac{\omega}{\gamma}$ is the n -th eigenvalue. Having solved this Schrödinger equation, we can compute the intensities I_n of each mode as³³

$$I_n \propto \frac{|\int_0^L m_n^+(z) dz|^2}{\int_0^L |m_n^+(z)|^2 dz}, \quad (8)$$

where the integration runs over the ferromagnetic film thickness.

B. Boundary conditions and intensity of SWR

To solve Eq. (6), it is crucial to establish the boundary conditions for SWR. While different boundary conditions do not affect the *positions* of the resonances in an essential way, the *intensity* of the SWR peaks strongly depends on them. It is therefore important to choose the appropriate boundary conditions (BCs).

The question of boundary conditions has been debated for a rather long time in the literature and, to our knowledge, no general agreement has been reached. Different authors^{34,35,36} treat the BC problem in different ways, and assume different boundary conditions appropriate to the specific sample which they are studying.

Equation (6) must be, in general, solved together with macroscopic Maxwell equations. Ament and Rado³⁷ argued that in the absence of any magnetic anisotropy the spin wave solutions should satisfy so-called free (or anti-node) boundary conditions ($\frac{dm^+(z)}{dz} = 0$ at $z = 0$ and $z = L$). On the other hand, Pincus³⁸ pointed out that Ament and Rado have not treated properly the discontinuity of the space at the surface of the film. Pincus (and also previously Kittel³⁹) indicated that at the interface an additional term, proportional to the gradient of the magnetization at the surface (not included in equation 6), is also allowed by symmetry, and that this term can lead to the pinning of spin waves at the boundaries. Furthermore, Pincus observed that free BCs can never be appropriate when there is surface anisotropy. He also showed that an antiferromagnetic oxide layer on the surface of a film can give rise to a surface anisotropy which pins the spins at the end-points ($m_n^+(z=0) = 0$ and $m_n^+(z=L) = 0$). Finally, Pincus and Kittel have shown that it is more appropriate to use the so-called *dynamic boundary conditions*,^{38,39} which for the lowest lying modes effectively reduce to pinned boundary conditions.

We believe that in the case of $\text{Ga}_{1-x}\text{Mn}_x\text{As}$ films one must also use *pinned* boundary conditions. This is because, first, there is a strong strain field present in these films that generates a large anisotropy field, and second, we expect a strong surface-induced anisotropy in the vicinity of the surface due to the strong spin-orbit coupling in $\text{Ga}_{1-x}\text{Mn}_x\text{As}$, which would also pin the spin waves⁴⁰. Fortunately, our numerical analysis allows us to try different boundary conditions. We were unable to obtain a good fit to the peak intensities when we used unpinned or partially unpinned boundary conditions. Pinned boundary conditions, on the other hand, gave very good agreement with the measured SWR spectra. This is illustrated in Fig. 4, where we show our best fits with pinned and unpinned boundary conditions for the SWR spectra for an as-grown 200 nm sample at $T = 4$ K.

Typical solutions for pinned boundary conditions and the corresponding intensities are shown in Fig. 5. The intensity of odd modes is suppressed, because of the can-

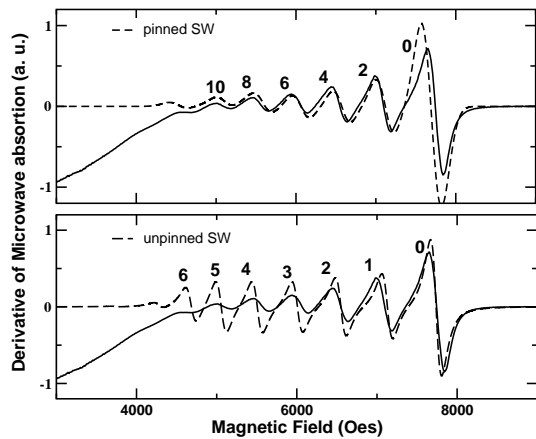


FIG. 4: The derivative of the absorption of the SWR as a function of applied dc magnetic field for an as-grown 200 nm $\text{Ga}_{1-x}\text{Mn}_x\text{As}$ film. The solid lines represent the experimental data, and the dashed lines show our theoretical results for the magnetic anisotropy profile of Eq. (9). The upper/lower panels show the results of our computations for pinned/unpinned boundary conditions.

cellation of the regions with $m^+ > 0$ and $m^+ < 0$, respectively. In fact, in Fig. 4 the odd modes are barely visible, and only peaks associated with the *even modes* can be observed.

The low energy spin (standing) waves tend to be localized around the region with higher magnetic anisotropy. Qualitatively speaking, this is because we have the *negative* of the spatially-dependent uniaxial anisotropy acting as the effective trapping potential for the modes, and therefore it is easier to create spin waves where the anisotropy is large. For smaller values of Λ , spin waves tend to be more localized around the large anisotropy points. On the other hand, spin waves with higher energies will be extended over the whole sample thickness, and their energy will not depend linearly on n .

IV. NUMERICAL RESULTS AND DISCUSSION

We solved Eq. (6) numerically, and varied the exchange parameter Λ and the profiles of the anisotropy field $H_a(z)$ (or the magnetization $M(z)$) to obtain a best fit to the experimental spectra. From these calculations we concluded that to explain a linear variation of the resonance fields, $H_n \sim n$, the changes of $H_a(z)$ (or $M(z)$) must be substantial across the whole depth of the sample. For profiles where the variation of $H_a(z)$ (or $M(z)$) is only near the surface, the resonance positions show always a quadratic behavior, $H_n \sim n^2$. This can be easily understood from Eq. (7), since in this case the potential $V(z)$ is similar to that of a rectangular quantum well and the eigen-modes are therefore quadratically separated.

As discussed in the previous section, the spatial variation of the magnetization and the exchange constant are

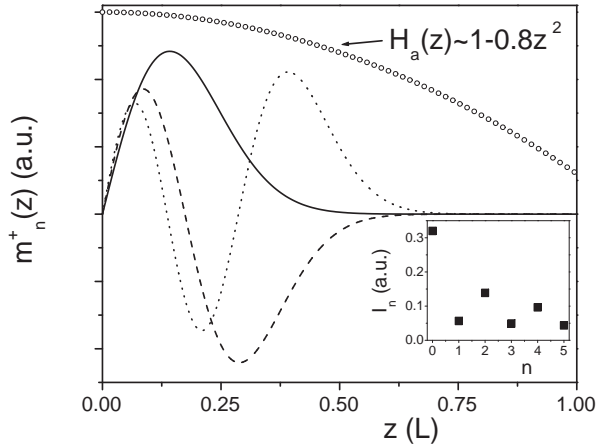


FIG. 5: Illustration of the functional form of three spin wave modes with $n = 0, 1$ and 2 (solid, dashed, and dotted lines) for the as-grown $L = 200$ nm sample at $T = 4$ K. We used an exchange constant $\Lambda = 3000$ nm² and $\alpha = 0.8$. The rescaled anisotropy profile is marked by open circles. Distances are measured in units of L . In the inset we show the calculated intensities I_n of the modes in the main figure .

sub-dominant processes. On the other hand, we were able to obtain quantitative agreement with the experimental data allowing the magnetic anisotropy field $H_a = H_a(z)$ to vary across the sample while keeping the magnetization constant, $M(z) = \text{const}$. Therefore, in the discussion that follows, we shall mostly focus to the case of a z -dependent anisotropy field, $H_a = H_a(z)$, and assume $M = \text{const}$.

The computed SWR spectrum depends on the specific shape of the anisotropy profile $H_a(z)$. We found, in particular, that a linear dependence of H_a on z , $H_a(z) \sim z$, is clearly in disagreement with our experimental data. However, we could obtain an excellent fit by assuming a quadratic dependence on z , $H_a(z) \sim z^2$. More specifically, both of the following profiles fit the experimental data rather well:

$$H_a(z) = H_a \exp(-\alpha z^2/L^2) \quad (9)$$

$$= H_a(1 - \alpha z^2/L^2), \quad (10)$$

where L is the thickness of the film, $\alpha \sim 0.75$ is a dimensionless fitting parameter, and the maximum value of the anisotropy field, $H_a(0)$, has been extracted from the analysis of the main FMR resonance⁵. Since we can obtain the value of the saturation magnetization M from accurate SQUID measurements, we end up with only two fitting parameters, α and the stiffness A (or equivalently, the exchange constant Λ).

The origin of the linear behavior on n can be easily understood from the formal analogy with the Schrödinger equation (Eq. 7) and the energy spectrum of the harmonic oscillator: as long as the difference between

the resonance field H_n and the maximum value of the anisotropy field $|H_a(0) - H_n|$ is small compared to $\frac{\omega_r}{\gamma}$, we expect the corresponding wave function $m^+(z)$ to be well approximated by the Hermite functions and to have a linear behavior $\sim n$. This condition is well satisfied for the experimentally observed spin wave resonance fields.

In order to study the anisotropy profile, we focused on the 200 nm sample, because this sample exhibited the largest number of resonance peaks. First, we chose our parameters to fit the 4 K data (Fig. 6): Having obtained the magnetization $M = 17.9$ emu/cm³ from SQUID experiments, and the magnetic anisotropy field $H_a = 4.400$ Oe from the angular dependence of the main FMR resonance line, we adjusted $\Lambda = 3000 \pm 300$ nm² and $\alpha = 0.75$ to obtain the best fit which corresponds to a spin stiffness $\mathbf{A} = 0.4$ meV/Å. For the spectrum measured at 40 K in the as-grown sample we obtained a very good fit with the *same* exchange constant Λ and α , but replacing $H_a(0)$ by the measured 40 K anisotropy $H_a^{40K}(0) = 4.200$ Oe and magnetization $M^{40K} = 9.4$ emu/cm³. In both cases the SWR spectra (and thus the resonance fields H_n) exhibit a *quasi-linear* dependence on n .

Annealing of Ga_{1-x}Mn_xAs has various - presently not entirely understood - effects. First, the saturation magnetization increases upon annealing. Furthermore, Rutherford backscattering experiments suggest⁴¹ that the primary process resulting from annealing is the diffusion of interstitial Mn ions out of the film. Since interstitial Mn takes away carriers from the hole band, annealing results probably in an *increase of the carrier density*, and the resulting carrier density is most likely *inhomogeneous*. Since both the anisotropy and the exchange energy are sensitive to the carrier density, annealing is expected to change the value of both H_a and Λ ,¹¹ and it may also change their profiles.

Consequently, it is natural to expect that the SWR

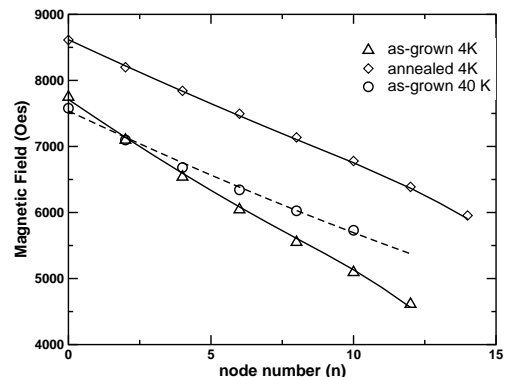


FIG. 6: Comparison between theoretical (solid lines) and experimental (symbols) data for the 200 nm sample. Two different temperatures for the as-grown sample and one temperature for the annealed sample are considered. The saturation magnetization data from SQUID measurements is included in the theoretical approach.

spectra observed on annealed specimens will require fitting parameters that are different from the ones used for the as-grown sample. Nevertheless, we were able to obtain a good fit to the experimental SWR by keeping the profile unchanged ($\alpha = 0.75$), adjusting the anisotropy field $H_a^{\text{anneal}}(0) = 5300$ Oe and using $\Lambda = 1225$ nm². Surprisingly, this value of exchange constant Λ corresponds to the same value of the stiffness parameter A as in the as-grown sample.

V. CONCLUSIONS

We have analyzed the experimental FMR and SWR spectra of thin Ga_{1-x}Mn_xAs films grown on GaAs substrates by low temperature MBE technique. We compared the experimentally observed resonance positions and intensities with theoretical calculations. The experimental results are clearly inconsistent with the assumption of a homogeneous Ga_{1-x}Mn_xAs film. After solving the semiclassical equations of motion and using independent experimental data for the magnetic anisotropy and magnetization, we have shown that a nearly quadratic z -dependence of the uniaxial anisotropy, $H_a(z) - H_a(0) \sim z^2$ could adequately explain the position and intensity of the experimental data. An inhomogeneous magnetization could also lead to similar effects. However, the spatial variation and the magnitude of magnetization needed to explain the experimental data is incompatible with the experiments. Spatial variation of the magnetization, as observed in Ref. 23 play a secondary role in the SWR spectra. From our numerical analysis we also concluded that the observed spin waves are pinned at the surfaces of the film. As a consequence of pinning, the intensity of $n = \text{odd}$ spin wave modes is suppressed and the experimentally observed spectra consist of even modes only.

Goennenwein *et al.* performed similar SWR measurements and also found spin wave spectra that are incompatible with having homogeneous Ga_{1-x}Mn_xAs films⁹. They, however, find that $H_n \propto n^{2/3}$, consistent with a linear z -dependence of the anisotropy field, $H_a(z) - H_a(0) \sim z$. This is in qualitative contrast with our findings for the resonance fields which scale as $H_n \sim n$. Furthermore, Goennenwein *et al.* appear to have implicitly assumed free boundary conditions, which implies that both even and odd modes are observable. In contrast, we argue that *pinned* boundary conditions are more adequate for our samples, and we find that, again, only even modes can be observed.

There may be several mechanisms that produce inhomogeneous magnetic parameters. The uniaxial anisotropy is primarily due to uniaxial strain field in the film that develops due to the lattice mismatch between the substrate and the ferromagnetic film^{5,10,11}. In principle, an inhomogeneous strain field could therefore produce an inhomogeneous anisotropy field H_a . However, in MBE grown samples the strain usually relaxes suddenly, when the sample reaches a critical thickness, where dislo-

cations start to form and relax the strain. In these non-equilibrium MBE grown samples, however, there seems to be no strain field relaxation at all through dislocation formation: Even for micron thick samples the measured in-plane lattice constant of the film is the same as that of the substrate.

One can also obtain inhomogeneous magnetic properties by assuming an inhomogeneous *hole concentration*. Indeed, annealing experiments support the notion that the dominant compensation effect is due to interstitial Mn ions, which act as double donors and may also compensate the spin of substitutional Mn. These interstitial Mn ions can diffuse out of the sample during the growth process, which takes usually a few hours and takes place at the same temperature as the annealing. As a result, it is quite possible that the concentration of charge carriers (related to that of Mn interstitials) varies across the film. Since the exchange anisotropy and exchange constants are both related to the carrier density³¹, this can serve as a mechanism to produce a z -dependent anisotropy field. Several recent experiments provide firm support for an inhomogeneous hole concentration: Koeder and coworkers³² find indications of gradients in both the carrier concentration and Curie temperature of epitaxial Ga_{1-x}Mn_xAs films. The presence of such gradients are also in accord with recent observations of interstitial Mn diffusion^{20,42}. The notion that Mn diffusion is a key process for annealing-induced enhancement of magnetism has recently been backed up by annealing experiments on samples *capped*⁴³ with a few monolayers of undoped GaAs, which would block the interstitial Mn from diffusing out of the sample. Under these circumstances the annealing process gave no significant increase in the Curie temperature. We believe that these experimental results, together with our resonance measurements and the theoretical arguments given above provide solid support for our calculation that a gradient in the magnetic parameters must be present in Ga_{1-x}Mn_xAs.

We also studied the linewidth of the observed resonances. For the as-grown samples the SWR linewidths do not depend on the mode number. This behavior hints that the relaxation is due to spin-orbit coupling.²⁷ Indeed, the measured (rather large) resonance width is compatible with the presence of a relatively large random anisotropy.

For the annealed samples, on the other hand, the linewidth decreases with increasing mode number, which is characteristic to eddy current relaxation in metallic samples¹⁹. This behavior is consistent with the results of annealing experiments, since for higher carrier densities the random anisotropy effects become less important, and at the same time the sample becomes more metallic. It also underscores the fact that there is a significant physical difference between as-grown and annealed samples, going beyond quantitative changes in the values of saturation magnetization and the Curie temperature.

Since the variation of elastic and/or magnetic proper-

ties across the $\text{Ga}_{1-x}\text{Mn}_x\text{As}$ film can have important consequences in its future spintronics applications, a more detailed experimental and theoretical analysis is necessary to understand and control the magnetic properties of these thin ferromagnetic layers. One way to obtain more information about the effects of the surface anisotropy is to perform FMR measurements in symmetric three-layer structures $\text{GaAs}/\text{Ga}_{1-x}\text{Mn}_x\text{As}/\text{GaAs}$ and compare them with the previously obtained results. A systematic study of the thickness and annealing time dependence of similarly grown samples would be also important to understand the origin of the observed gradient of composition.

VI. ACKNOWLEDGMENT

We would like to thanks Prof. John B. Ketterson for important comments. This research was supported by the National Science Foundation under NSF-NIRT award DMR 02-10519, by the U.S. Department of Energy, Basic Energy Sciences, under Contract No. W-7405-ENG-36, by the Alfred P. Sloan Foundation (B.J.), and by the NSF and Hungarian Grants No. OTKA F030041, and T038162. G.Z. is a Bolyai Fellow of the Hungarian Academy of Sciences.

-
- ¹ H. Ohno, *Science* **281**, 951 (1998).
- ² J. K. Furdyna, S. Schiffer, P. and Sasaki, J. Potashnik, and X. Y. Liu, *Optical Properties of Semiconductor Nanostructures*, vol. 81 (NATO Science Series, 2000).
- ³ H. Ohno, *J. Magn. Magn. Mater.* **242**, 105 (2002).
- ⁴ M. Farle, *Rep. Prog. Phys.* **61**, 755 (1998).
- ⁵ X. Liu, Y. Sasaki, and J. K. Furdyna, *Phys. Rev. B* **67**, 205207 (2003).
- ⁶ O. Fedorych, M. Byszewska, Z. Wilamowski, M. Potemski, and J. Sadowski, *Acta Phys. Pol. A* **102**, 617 (2002).
- ⁷ C. Kittel, *Phys. Rev* **110**, 1295 (1958).
- ⁸ The stiffness D is related to the constant A in Section III as $D = 2A/M$ where M is the magnetization.
- ⁹ S. T. B. Goennenwein *et al.*, *Appl. Phys. Lett.* **82**, 730 (2003).
- ¹⁰ H. Ohno, A. Shen, F. Matsukura, A. Oiwa, A. Endo, S. Katsumoto, and Y. Iye, *Appl. Phys. Lett.* **69**, 363 (1996).
- ¹¹ M. Abolfath, T. Jungwirth, and A. H. MacDonald, *Physica E* **10**, 161 (2001).
- ¹² T. Dietl, J. Konig, and A. H. MacDonald, *Phys. Rev. B* **64**, 241201 (2001).
- ¹³ Y. Sasaki, X. Liu, J. K. Furdyna, M. Palczewska, J. Szczytko, and A. Twardowski, *J. Appl. Phys.* **91**, 7484 (2002).
- ¹⁴ A. Kaminski and S. D. Sarma, *Phys. Rev. Lett.* **88**, 247202 (2002).
- ¹⁵ M. Berciu and R. N. Bhatt, *Phys. Rev. Lett.* **87**, 107203 (2001).
- ¹⁶ G. A. Fiete, G. Zarand, and K. Damle, *Phys. Rev. Lett.* **91**, 097202 (2003).
- ¹⁷ Y. Sasaki, X. Liu, and Furdyna, *J. Supercond.* **16**, 41 (2003).
- ¹⁸ The intensity of a resonance can be modelled as $I(H) = (I_0/\Delta H)f(H/\Delta H)$ where the total integrated intensity is I_0 , and $\int_{-\infty}^{+\infty} dx f(x) = 1$. Then the peak-to-peak change in the derivative of the intensity is $\Delta I = |f'(1/2)(I_0/\Delta H^2)$.
- ¹⁹ G. Rado and W. Asment, *Phys. Rev.* **97**, 1558 (1955).
- ²⁰ K. M. Yu, W. Walukiewicz, T. Wojtowicz, I. Kuryliszyn, X. Liu, Y. Sasaki, and J. K. Furdyna, *Phys. Rev. B* **65**, 201303 (2002).
- ²¹ Y. Sasaki, P.h.D Thesis University of Notre Dame (2002).
- ²² Portis, *Appl. Phys. Lett.* **2**, 69 (1963).
- ²³ J. Rhyne, B. Kirby, S. teVelthuis, A. Hoffmann, T. Wojtowicz, X. Liu, and J. Furdyna, (unpublished).
- ²⁴ In Fig.3.c the theoretical results, shown as point connected by dashed lines, for the normalized mode intensity were calculated within a model where the anisotropy has a quadratic dependence on the distance from the interface. For more realistic model of anisotropy variation, see Section IV.
- ²⁵ T. Dietl, H. Ohno, F. Matsukura, J. Cibert, and D. Ferrand, *Science* **287**, 1019 (2000).
- ²⁶ T. Jungwirth, J. Konig, J. Sinova, J. Kucera, and A. H. MacDonald, *Phys. Rev. B* **66**, 012402 (2002).
- ²⁷ G. Zarand and B. Janko, *Phys. Rev. Lett.* **89**, 47201 (2002).
- ²⁸ J. Schliemann and A. H. MacDonald, *Phys. Rev. Lett.* **88**, 137201 (2002).
- ²⁹ U. Welp, V. K. Vlasko-Vlasov, X. Liu, J. F. Furdyna, and T. Wojtowicz, *Phys. Rev. Lett.* **90**, 167206 (2003).
- ³⁰ L. Landau and E. Lifshitz, *Physik. Z. Sowjetunion* **8**, 153 (1935).
- ³¹ M. Abolfath, T. Jungwirth, J. Brum, and A. H. MacDonald, *Phys. Rev. B* **63**, 054418 (2001).
- ³² A. Koeder *et al.*, *Appl. Phys. Lett.* **82**, 3278 (2003).
- ³³ M. Sparks, *Phys. Rev B* **1**, 3869 (1970).
- ³⁴ B. Hoekstra, R. P. van Stapele, and J. M. Robertson, *J. Appl. Phys.* **48**, 382 (1977).
- ³⁵ M. Sparks, *Phys. Rev. Lett* **22**, 1111 (1969).
- ³⁶ R. F. Soohoo, *Phys. Rev* **131**, 594 (1963).
- ³⁷ W. S. Ament and G. T. Rado, *Phys. Rev. B* **97**, 1558 (1955).
- ³⁸ P. Pincus, *Phys. Rev. B* **118**, 658 (1960).
- ³⁹ C. Kittel, *Revs. Modern Phys.* **21**, 541 (1949).
- ⁴⁰ O. Ujsaghy, A. Zawadowski, and B. L. Gyorffy, *Phys. Rev. Lett.* **76**, 2378 (1996).
- ⁴¹ K. Yu, W. Walukiewicz, T. Wojtowicz, I. Kuryliszyn, X. Liu, Y. Sasaki, and F. J.K., *Phys. Rev. B* **65**, 201303 (2002).
- ⁴² B. L. Gallagher *et al.*, cond-mat/0307140.
- ⁴³ M. Stone, K. Ku, S. J. Potashnik, B. L. Sheu, N. Samarth, and P. Schiffer, cond-mat/0307255.